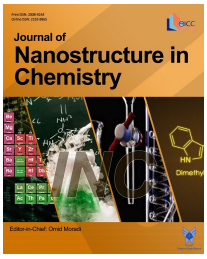

Volume 15, Issue 5, 152518 (1-11)

Journal of Nanostructure in Chemistry (JNSC)

https://doi.org/10.57647/jnsc.2025.1505.18

A High-Sensitivity Sensor with Simultaneous Enhanced Effect with Ionic Liquid and NiO/SWCNTs Catalysts to Create High-Performance Conditions for Vanillin Measurement

Ebrahim Halalkhor-Mirkolayi[1], Azade Ghorbani-HasanSaraei[1,*], Mohammad Bagher Limooei[2], Peiman Ariaii[1], Seyed-Ahmad Shahidi[1]

[1]*Department of Food Science and Technology, Am.C., Islamic Azad University, Amol, Iran.*
[2]*Department of Materials Science and Engineering, Am.C., Islamic Azad University, Amol, Iran.*

[*]**Corresponding author:** az.ghorbanihasansaraei@iau.ac.ir

Original Research

Received:
22 August 2025
Revised:
28 September 2025
Accepted:
8 October 2025
Published online:
15 October 2025

Abstract:

Paying attention to the quality of food products and examining its additives, as well as controlling their concentration, are among the most important issues in the food industry. Therefore, various methods of measuring food additives have been proposed in recent years. The present study designed and investigated the performance of an electrochemical sensor prepared with carbon paste (CP) that was simultaneously modified using NiO/SWCNTs nanocomposite and ionic liquid (1-Hexyl-3-methylimidazolium tetrafluoroborate; [HMIM][BF_4]), and evaluated its effect on the oxidation signal of vanillin in food samples. The NiO/SWCNTs nanocomposite was synthesized as conductive catalyst with high surface area by chemical precipitation method and characterized by SEM and MAP analysis. The presence of the NiO/SWCNTs nanocomposite and [HMIM][BF_4] increased the oxidation current by 3.22 times and reduced the vanillin oxidation overvoltage by 225 mV, indicating the synergistic role of the two catalysts in the construction of the NiO/SWCNTs/[HMIM][BF_4]/PE. The effective parameters such as type of buffer, pH, percentage of catalysts were optimized and results showed phosphate buffer (pH = 6.0) can be use as optimum condition in monitoring process. In addition, 20% (v:v) of [HMIM][BF_4] and 15% (w:w) of NiO/SWCNTs were selected as optimum condition for fabrication of NiO/SWCNTs/[HMIM][BF_4]/PE. The NiO/SWCNTs/[HMIM][BF_4]/PE showed a detection limit 0.3 nM for monitoring of vanillin. In the final stage, NiO/SWCNTs/[HMIM][BF_4]/PE was used for monitoring of vanillin in different food samples such as biscuit, chocolate and coffee milk with acceptable recovery data.

Keywords: NiO/SWCNTs nanocomposite; Vanillin; 1-Hexyl-3-methylimidazolium tetrafluoroborate; Electrochemical sensor; Food analysis

Cite this article: Halalkhor-Mirkolayi, E., Ghorbani-HasanSaraei, A., Limooei, M.B., Ariaii, P., Shahidi, S.-A. A High-Sensitivity Sensor with Simultaneous Enhanced Effect with Ionic Liquid and NiO/SWCNTs Catalysts to Create High-Performance Conditions for Vanillin Measurement. *J Nanostruct Chem* **15**(5), 152518 (2025).

1. Introduction

Paying attention to nutrition and food safety is considered as one of the ways to prevent widespread diseases, as well as reduce treatment costs and increase public health [1, 2]. Many strict rules are applied to the types of additives and also to determine their concentration in different food samples in developed countries [3, 4]. Food quality certainly affects the health of the community and has a significant impact on reducing dangerous diseases such as cancer [5, 6]. Accordingly, quality control and determination of food additives are incorporated in all food quality control laboratories. Vanillin, a widely used flavoring, occurs naturally in the seeds of the vanilla plant (Vanilla planifolia), but the majority consumed industrially is produced synthetically, typically from petroleum or lignin-derived compounds [7].

Regulatory bodies have evaluated its safety: the U.S. Food and Drug Administration (FDA) lists vanillin as "generally recognized as safe" (GRAS) for use in foods, while the European Food Safety Authority (EFSA), following JECFA, has established an acceptable daily intake (ADI) of $0-10$ mg per kg body weight. These regulatory guidelines confirm that vanillin is safe at the permitted concentrations typically used in food products [8–10]. However, it's excessive or continuous consumption, or under certain conditions, can have some disadvantages or concerns, including allergic problems, irritation of the digestive system, and possible effects on the liver and kidney [11, 12]. Accordingly, determining its accurate concentration in food samples is very important and necessary to reduce adverse effects [13, 14]. There have been various reports of different measurement methods for vanillin in recent years, which indicate the importance of paying attention to determining its amount in food samples [15–18].

Electrochemical methods are known as one of the rapid measurement methods with low cost and low contamination as a suitable method for the analysis of food and biological contaminants [19–21]. Several reports of the use of electrochemical methods for the measurement of vanillin have been presented, which confirms the ability of this method for the analysis of food materials [22, 23]. The weak signal and high overvoltage of the compounds measured in electrochemical methods have necessitated the need to modify the electrode surface to improve the efficiency of the method [24–28]. Vanillin is not exempt from this issue and enabling and improving electrode surfaces for its measurement at low concentrations seems important and necessary [29]. Modification of electrode surfaces to create a sensitive and selective system using various catalysts is growing and flourishing [30, 31]. Nanomaterials have become an integral part of electrode surface modifiers. Carbon-based nanomaterials such as graphene, carbon nanotubes, MXene, as well as metal and metal oxide nanoparticles such as platinum, gold, nickel oxide, zinc oxide have well proven their ability to improve the conductivity of electrode surfaces [32–34]. The remarkable properties of this class of compounds have led to incredible changes in most branches of engineering [35]. There are numerous reports of the amazing effects of carbon/metal nanocomposites for improving the electrical properties of surfaces in electrochemical systems [36].

Ionic liquids are another catalyst used in electrochemical systems, and due to their unique structure and conductivity due to their structural charges, they have been used as a suitable option in modifying electrode surfaces [37, 38]. The increased electrical conductivity caused by ionic liquids can reduce overvoltage and improve the efficiency of electrochemical sensors. This is especially true when using carbon paste electrodes. Simply replacing the electrode with bonding oil with good electrical conductivity can greatly increase the performance of these types of electrodes.

Considering the above points regarding the importance of vanillin measurement and the capabilities of electrochemical sensors, especially modified sensors, this research work designed and presented a modified electrochemical sensor with carbon paste and used NiO/SWCNTs nanocomposite and [HMIM][BF_4] (scheme 1) to improve its efficiency, in order to provide a suitable solution for measuring small amounts of vanillin, considering the existing synergistic effects. The NiO/SWCNTs/[HMIM][BF_4]/PE was selected as a new tool for monitoring of vanillin in food samples with acceptable results.

Although a previous study reported the design of an electrochemical sensor based on NiO/SWCNT nanocomposites for vanillin monitoring, the present work employed a different ionic liquid, [HMIM][BF_4], instead of 1-butylpyridinium hexafluorophosphate used in the earlier report [42]. This modification led to a lower detection limit, which can be attributed to the higher ionic conductivity of [HMIM][BF_4] compared to 1-butylpyridinium hexafluorophosphate. Table 1 presents a comparison of the proposed sensor with previously reported systems, clearly demonstrating the superior performance and high capability of the designed sensor.

2. Experimental

2.1 Methods, instrument and materials

Nickel (II) nitrate hexahydrate, single-walled carbon nanotubes, and sodium hydroxide were obtained from Sigma-Aldrich and utilized in the synthesis of NiO/SWCNTs using a chemical precipitation method previously reported by our research group. Graphite powder, paraffin oil, diethyl ether and [HMIM][BF_4] were purchased from Sigma-Aldrich and Merck Company and used form fabrication

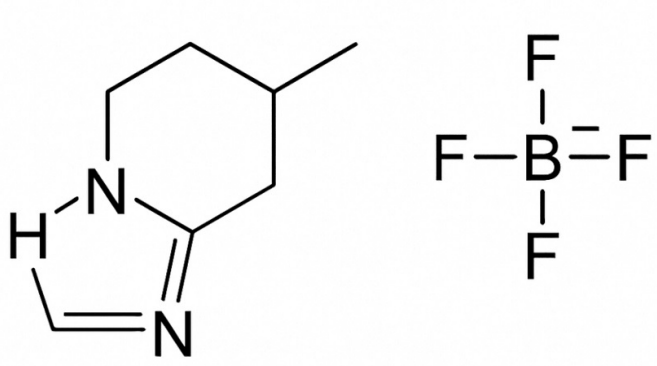

Scheme 1. Structure of 1-Hexyl-3-methylimidazolium tetrafluoroborate.

Table 1. Analytical parameters reported for electrochemical monitoring of vanillin.

Electrode	Modifier	LDR (μM)	LOD (μM)	Ref.
Glassy carbon electrode	Multi-walled carbon nanotubes	4.15 – 294.12	0.0085	[39]
Graphene paste electrode	Ionic surfactant	4.0 – 70	1.29	[40]
Carbon paste electrode	MgO/SWCNTs + 1-butyl-3-methylimidazolium hexafluoro phosphate	0.02 – 800	0.008	[41]
Carbon paste electrode	NiO-SWCNTs + 1-butylpyridinium hexafluorophosphate	0.01 – 350	0.007	[42]
Acetylene black paste electrode	graphene–polyvinylpyrrolidone composite film	0.02 – 100	0.01	[43]
Glassy carbon electrode	Graphene film	0.6 – 48	0.056	[44]
Carbon paste electrode	NiO/SWCNTs + [HMIM][BF4]	0.001 – 350	0.0003	This work

of sensor. Vanillin was purchased from Across Company, and a standard solution was prepared by dissolving 0.38 g of vanillin in 25 mL of phosphate buffer solution (pH = 6.0) for all experimental signals. Acetic acid, phosphoric acid, boric acids were purchased from Merck Company and use for preparation of acetate buffer, phosphate buffer and Britton–Robinson buffer. Electrochemical signals were recorded using an Ivium-Vertex device, and all signals are shown based on an Ag/AgCl/KClsat reference electrode. A Pt wire was selected as the counter electrode, and NiO/SWCNTs/[HMIM][BF_4]/PE was also used as the working electrode. The 913 pH Meter (Metrohm, Switzerland) was used to prepare different buffers and adjust the pH values. Field emission scanning electron microscopy (FE-SEM) images were obtained using a Zeiss GeminiSEM 500 operated at an accelerating voltage of 3.0 kV.

2.2 Fabrication of NiO/SWCNTs/[HMIM][BF_4]/PE

After optimizing the effective factors, the NiO/SWCNTs/[HMIM][BF_4]/PE was prepared by mixing 0.85 g of graphite powder ($\sim$ 20 μm average particle size) and 0.15 g of the nanocomposite in a mortar and pestle, with diethyl ether used as a solvent. To create a uniform paste, paraffin oil and ionic liquid were slowly added to the sample in a volume ratio of 8:2, and the mixture was stirred. The black paste was added to the end of a glass tube, and a copper wire was submerged to the bottom as an electrical contact between the conductive carbon paste and the external measurement circuit (potentiostat/galvanostat).

2.3 Real sample preparation

Chocolate, Coffee milk and biscuits were selected as vanillin sources in food samples and were acquired to evaluate the effectiveness of NiO/SWCNTs/[HMIM][BF_4]/PE in analyzing vanillin in actual samples. A total of five samples were sourced from the local market and ground using a mortar and pestle. Half a gram of the powdered samples or 0.5 mL of coffee was mixed with 5 mL of ethanol and sonicated for one hour. The resulting mixtures, which included the vanillin extract, were then centrifuged at 6000 rpm for 20 minutes and used directly for vanillin quantification via the standard addition method [42].

3. Results and discussion

3.1 Optimization of effective factors

In the NiO/SWCNTs/[HMIM][BF_4]/PE design section, we evaluated the percentages of NiO/SWCNTs relative to graphite powder and [HMIM][BF_4] relative to paraffin oil as two key determining factors. To achieve this, carbon paste electrodes were prepared with varying volume percentages of [HMIM][BF_4] and paraffin oil ($0-30\%$ v:v), and the vanillin signal was recorded on the surface of each electrode. The results are presented in figure 1 (A). As shown, increasing the percentage of [HMIM][BF_4] from 0 to 20% resulted in a rise in the vanillin signal due to enhanced surface conductivity, followed by a sharp decline caused by a greasy layer of [HMIM][BF_4] forming on the electrode surface, which hindered direct contact between vanillin and the electrode. Consequently, 20% of the ionic liquid was selected as the optimal condition for sensor design. In the next step, we recorded the changes in sensor current in the presence of 500 μM of vanillin on the surface of the NiO/SWCNTs/PE with nanocatalyst percentages ranging from 0 to 20%. The results are shown in figure 1 (B).

Notably, as the percentage of NiO/SWCNTs increased to 15% (w:w), the vanillin oxidation signal increased before stabilizing. This trend is attributed to the NiO/SWCNTs nanocomposite's ability to enhance the conductivity of the electrode surface. Beyond this percentage, the conductivity became saturated, leading to a stable current.

Given the importance of pH factor, its role and type were evaluated. For this purpose, three types of buffers (acetate buffer (ionic strength $\approx$ 0.1 M), phosphate buffer (ionic strength $\approx$ 0.15 M) and Britton–Robinson buffer (ionic strength $\approx$ 0.2 M)) that are capable of creating pH 6 were selected. The changes in the vanillin signal were recorded under optimal conditions in the solution of these three buffers and the results showed that phosphate buffer can provide the best efficiency in vanillin analysis (figure 1 (C)). Next, we investigated how the vanillin signal varies with changes in the pH of the phosphate buffer solution, and the results are presented in figure 2. Linear sweep voltammograms of 500 μM vanillin in the pH range of 3.0 to 7.0 are shown in the inset of figure 2. A negative shift in potential was observed with increasing pH values (slope 63 mV/pH), confirming that the redox reaction of vanillin is controlled by proton

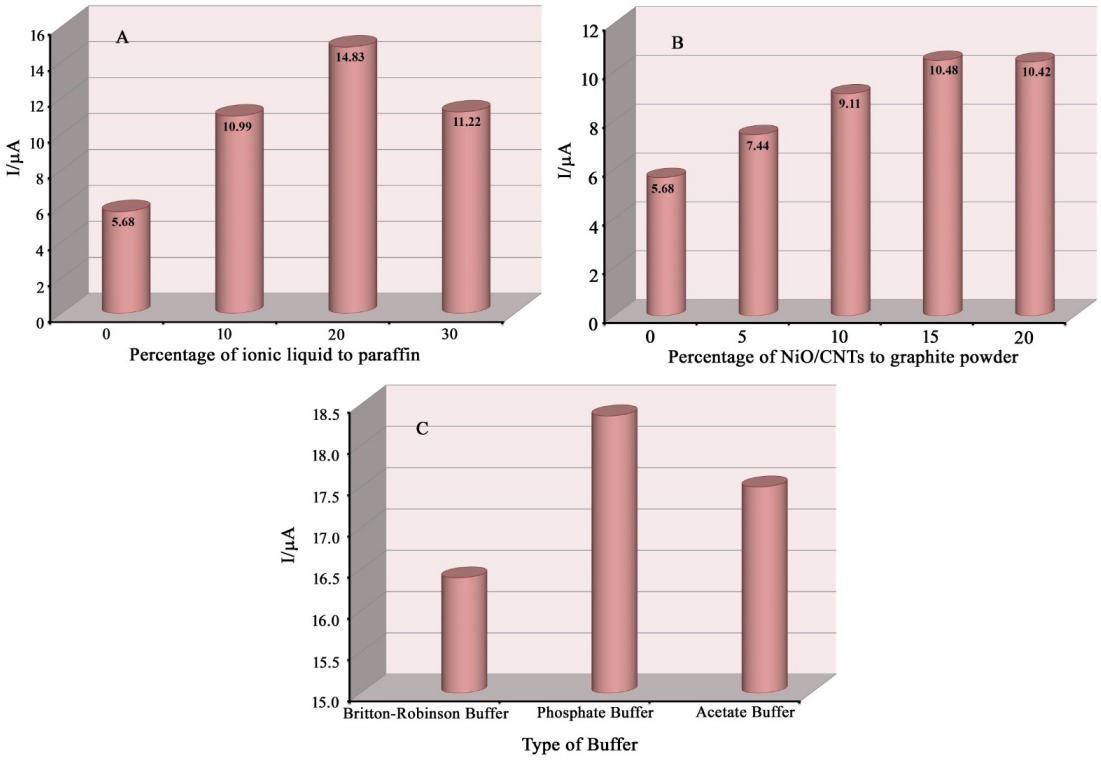

Figure 1. (A) Diagram of the oxidation current of vanillin recorded on the surface of [HMIM][BF_4]/PE prepared with varying ratios of [HMIM][BF_4]. (B) Diagram of the oxidation current of vanillin recorded on the surface of NiO/SWCNTs/PE prepared with different percentages of NiO/SWCNTs. (C) Diagram of the oxidation current of vanillin recorded on the surface of NiO/SWCNTs/[HMIM][BF_4]/PE in various types of buffer at pH 6.0.

changes. The recorded slope closely matches the recommended value for the equality of electrons and protons in the redox reaction of vanillin (scheme 2) [45]. On the other hand, maximum oxidation current for 500 µM vanillin at surface of NiO/SWCNTs/[HMIM][BF_4]/PE was detected at pH = 6.0 and this condition was selected as best electroanalytical condition for monitoring of vanillin in next steps.

3.2 NiO/SWCNTs characterization

The scanning electron microscopy (SEM) images of NiO/SWCNTs reveal a fascinating and intricate nanostructure (see figure 3). At various magnifications, you can see how the single-walled carbon nanotubes (SWCNTs) intertwine with nickel oxide (NiO) particles, creating a unique and interconnected network. This uniform distribution of NiO on the SWCNTs is essential for boosting the material's electrocatalytic properties. The porous structure highlighted in the images suggests a larger surface area, which

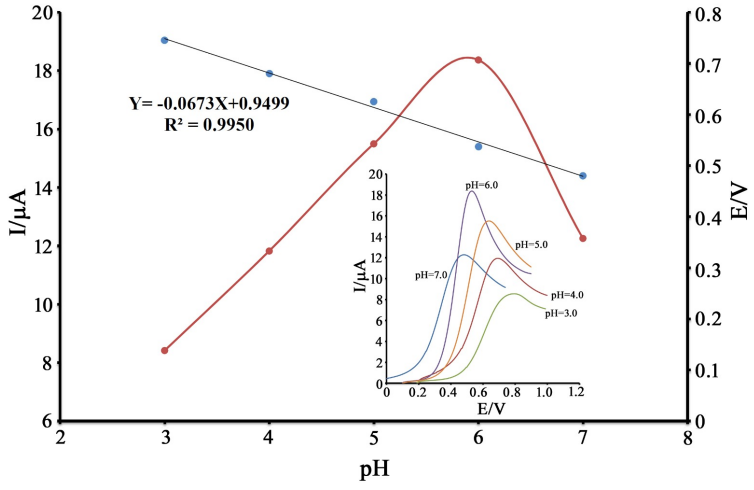

Figure 2. Current (red points) and potential (blue points) changing vs. pH for electro oxidation 500 µM vanillin in the pH range of 3.0 to 7.0. Inset. Linear sweep voltammograms of 500 µM vanillin in the pH range of 3.0 to 7.0.

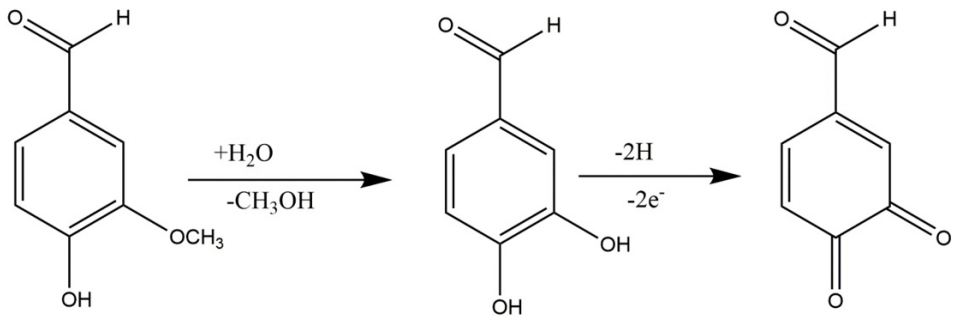

Scheme 2. Electrochemical oxidation mechanism of vanillin.

enhances interaction with the analyte during electrochemical reactions. Overall, these features showcase the promise of NiO/SWCNTs for use in sensors and other electrochemical applications, pointing to exciting possibilities in the field.

The multiphase analysis (MAP) and EDS images of the NiO/SWCNTs composite provide valuable insight into its elemental composition (figure 4). The top image provides an overview, showing a vibrant mix of carbon, nitrogen, oxygen, and nickel throughout the material. In the detailed maps below, the carbon (C) is highlighted in a strong red, showcasing the abundance of single-walled carbon nanotubes (SWCNTs), while the nitrogen (N) appears more subdued, indicating it's present in smaller amounts that can be relative to impurities resulting from insufficient washing of the sediment. The oxygen (O) map reveals the incorporation of nickel oxide, which plays a vital role in boosting the composite's electrochemical properties. Lastly, the nickel (Ni) map shows that the NiO is evenly distributed, reinforcing the composite's effectiveness. The EDX analysis of NiO/SWCNTs shows carbon as the major component (95.29 wt%), confirming the dominant SWCNT framework. Oxygen (3.35 wt%) and nickel (1.36 wt%) indicate the successful incorporation of NiO nanoparticles. The low oxygen

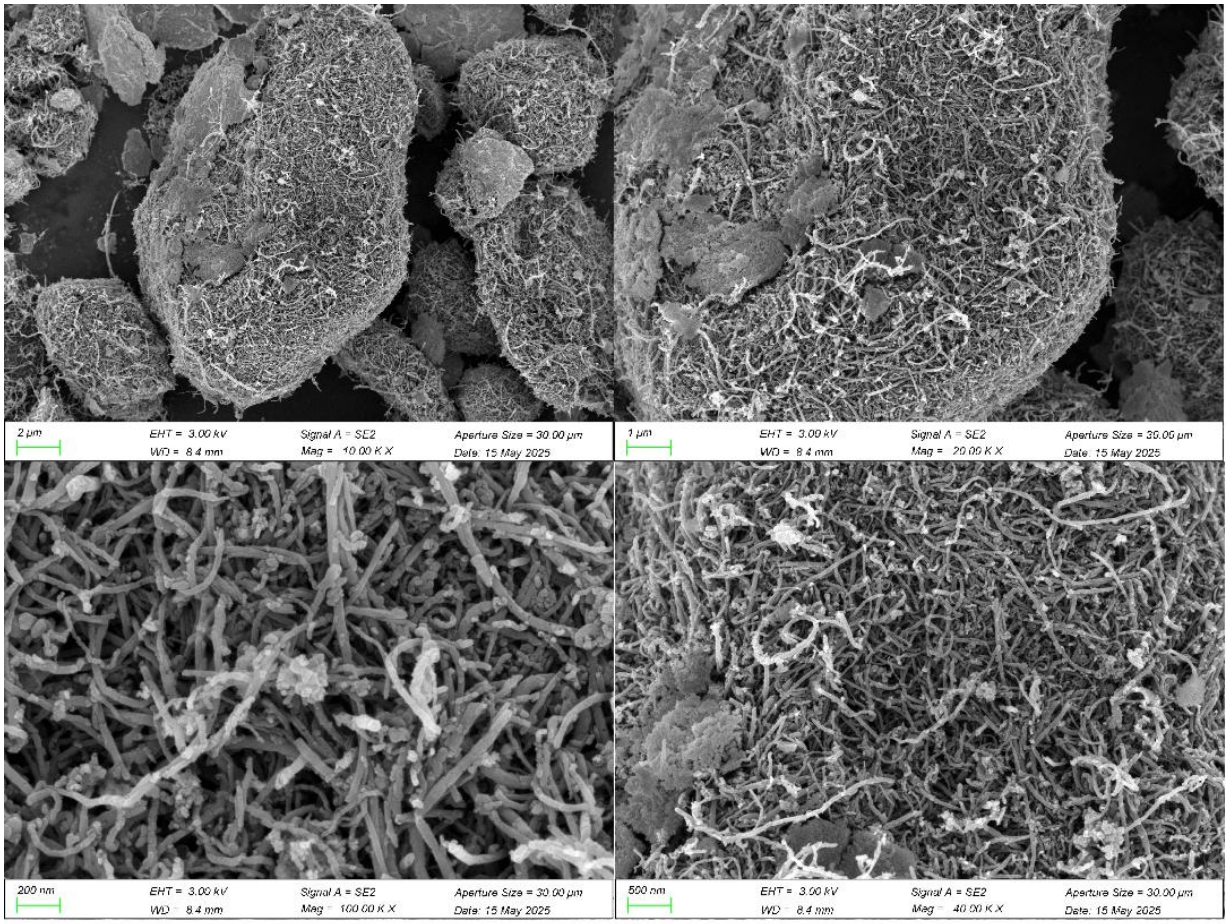

Figure 3. SEM images of NiO/SWCNTs with various magnifications.

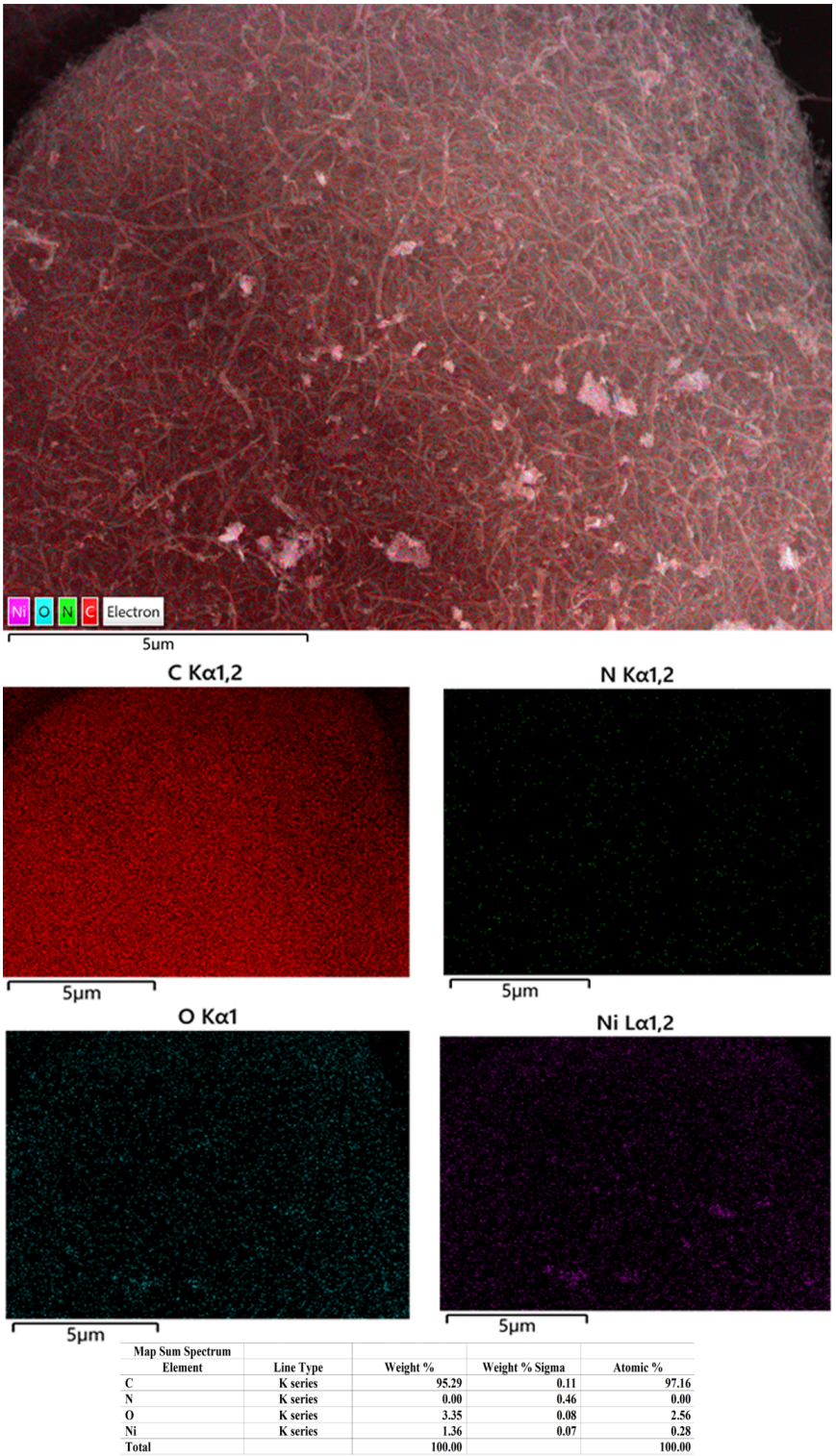

Map Sum Spectrum Element	Line Type	Weight %	Weight % Sigma	Atomic %
C	K series	95.29	0.11	97.16
N	K series	0.00	0.46	0.00
O	K series	3.35	0.08	2.56
Ni	K series	1.36	0.07	0.28
Total		100.00		100.00

Figure 4. MAP distribution diagram and EDS analysis (inset) of NiO/SWCNTs nanocomposite.

level suggests minimal oxidation, preserving CNT conductivity, while dispersed NiO provides redox-active sites. This composition highlights the synergistic role of SWCNTs as a conductive network and NiO as catalytic centers, beneficial for electrochemical applications.

The crystalline structure of the NiO/SWCNTs composite was investigated by XRD analysis (figure 5). The broad diffraction feature observed in the range of $20-26°$ corresponds to the (002) plane of graphitic carbon, confirming the presence of SWCNTs. In addition, the distinct diffraction peaks appearing at approximately 37.2°, 43.3°, 62.9°, and 75.4° can be indexed to the (111), (200), (220), and (311) planes of cubic NiO (JCPDS card No. 47-1049), respectively. The coexistence of these peaks demonstrates the successful integration of NiO nanoparticles with the SWCNT matrix. The absence of any additional reflections indicates that no crystalline impurities were formed during synthesis. Moreover, the relatively broad nature of the

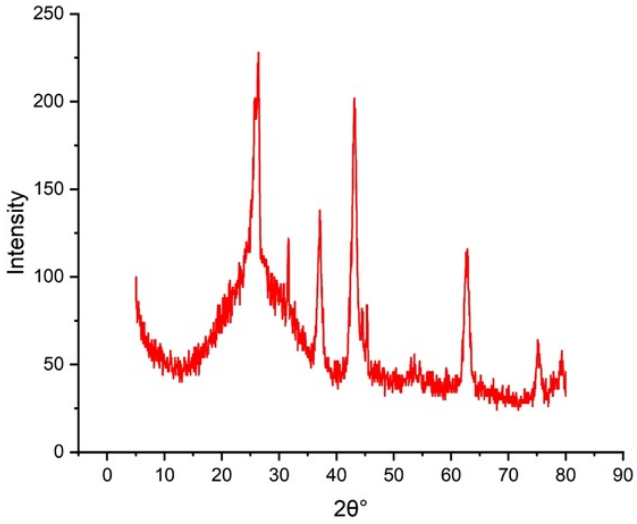

Figure 5. XRD pattern of NiO/SWCNTs composite.

NiO peaks suggests the nanoscale crystallite size of NiO, which is favorable for enhancing the active surface area and electron transfer efficiency in electrochemical applications.

3.3 Electrochemical investigation

The linear sweep voltammograms of 500 µM vanillin were recorded at the surface of different electrodes: PE (curve a), NiO/SWCNTs/PE (curve b), [HMIM][BF_4]/PE (curve c), and NiO/SWCNTs/[HMIM][BF_4]/PE (curve d) (figure 6 (A)). The results showed oxidation currents and potentials of 5.68 µA at 750 mV for curve a, 10.84 µA at 640 mV for curve b, 14.83 µA at 615 mV for curve c, and 18.32 µA at 525 mV for curve d. Comparing the data obtained from the carbon paste electrode with that from the modified electrode reveals a 225 mV decrease in potential and a 3.22-fold increase in current. This significant change confirms the synergistic effect of the modification, enhancing sensitivity in the measurement of vanillin.

The active surface areas of the unmodified and modified electrodes were calculated using the Randles–Sevcik equation, yielding values of 0.11 cm^2, 0.15 cm^2, 0.17 cm^2, and 0.19 cm^2 for PE, NiO/SWCNTs/PE, [HMIM][BF_4]/PE, and NiO/SWCNTs/[HMIM][BF_4]/PE, respectively. Based on these surface areas, the corresponding current density diagrams for the four electrodes are presented in figure 6 (B), which clearly demonstrate the enhanced electrochemical activity of both catalysts as well as their synergistic effect in the modification process.

The changes in the vanillin redox process were investigated by varying the potential scan rate at the NiO/SWCNTs/[HMIM][BF_4]/PE surface, using scan rates ranging from 15 to 100 mV/s, as shown in the inset of figure 7 inset.

The cyclic voltammograms exhibited irreversible behavior

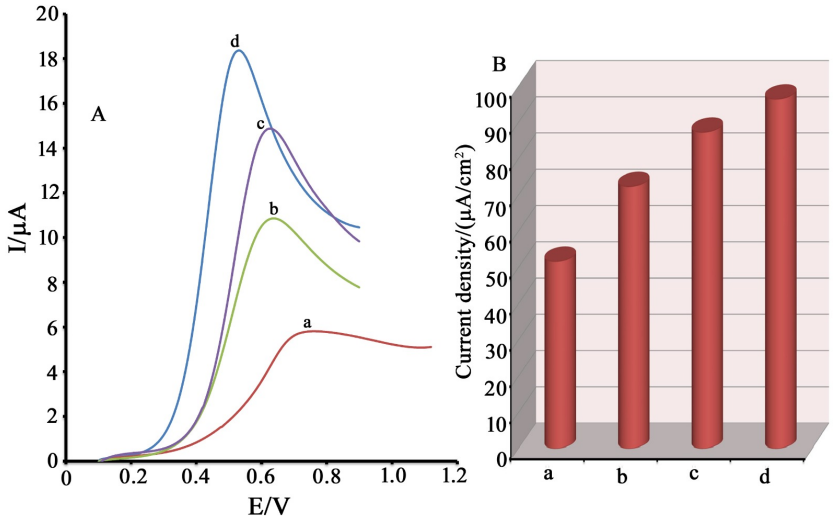

Figure 6. (A) Linear sweep voltammograms of 500 µM vanillin at surface of PE (a), NiO/SWCNTs/PE (b), [HMIM][BF_4]/PE (c), and NiO/SWCNTs/[HMIM][BF_4]/PE (d). (B) Current density results for 500 µM vanillin at surface of PE (a), NiO/SWCNTs/PE (b), [HMIM][BF_4]/PE (c), and NiO/SWCNTs/[HMIM][BF_4]/PE (d).

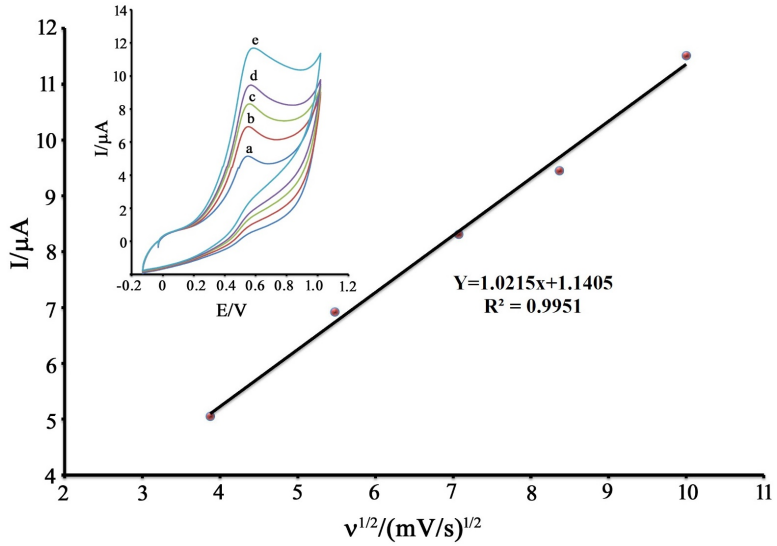

Figure 7. Current-$\nu^{1/2}$ curve for redox reaction of 300 μM vanillin at surface of NiO/SWCNTs/[HMIM][BF_4]/PE. Inset) Cyclic voltammograms of 300 μM vanillin at surface of NiO/SWCNTs/[HMIM][BF_4]/PE in scan rate (a) 15; (b) 30; (c) 50; (d) 70 and (e) 100 mV/s.

at all scan rates, along with a positive shift in oxidation potential as the scan rate increased. This observation confirms the kinetic limitations in the redox reaction of vanillin. Furthermore, the changes in vanillin oxidation current, plotted against the square root of the potential sweep rate, exhibited a linear relationship represented by the equation $I = 1.0215\nu^{1/2} + 1.1404$ ($R^2 = 0.9951$). This finding confirms that the vanillin redox process is governed by the diffusion of the analyte from the solution to the electrode surface.

To explain the rate-determining step, a Tafel plot was constructed using data points from the Tafel region of the linear sweep voltammogram (figure 8). The slope was determined to be 0.1260 V/dec at a scan rate of 50 mV/s, consistent with the theoretical value of $2.3RT/n(1-\alpha)F$, yielding an electron transfer coefficient (α) of 0.76.

Chronoamperometric experiments for vanillin at the NiO/SWCNTs/[HMIM][BF_4]/PE were conducted by fixing the working electrode potential at 0.8 V (not shown). For an electroactive analyte such as vanillin, the diffusion-controlled current response follows the Cottrell equation [46]. Accordingly, experimental plots of current (I) versus $t^{-1/2}$ were obtained for different vanillin concentrations. The resulting linear slopes were then correlated with vanillin concentration. Based on the slope values and the Cottrell equation, the diffusion coefficient (D) of vanillin was calculated 2.0×10^{-6} cm^2/s.

3.4 Analytical parameters

The analytical capability of the designed sensor and its important factors were investigated using differential pulse voltammetry (DPV). For this purpose, differential pulse voltammograms of vanillin were recorded in the linear range of 1.0 nM to 350 μM and the data obtained from the oxidation current of this compound showed a linear relationship with the equation $I = 0.1203C + 3.1670$ ($R^2 = 0.9939$) with respect to the concentration changes (figure 9).

The detection limit 0.3 nM was detected for monitoring

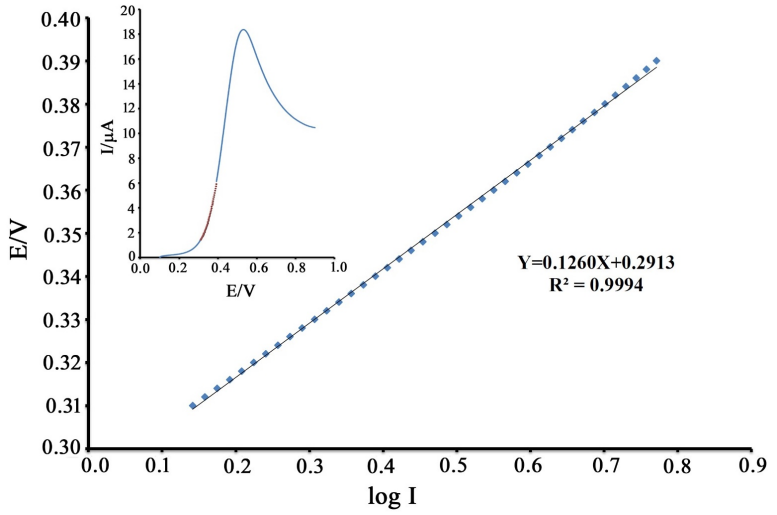

Figure 8. Talef plot of NiO/SWCNTs/[HMIM][BF_4]/PE in the presence of 500 μM vanillin.

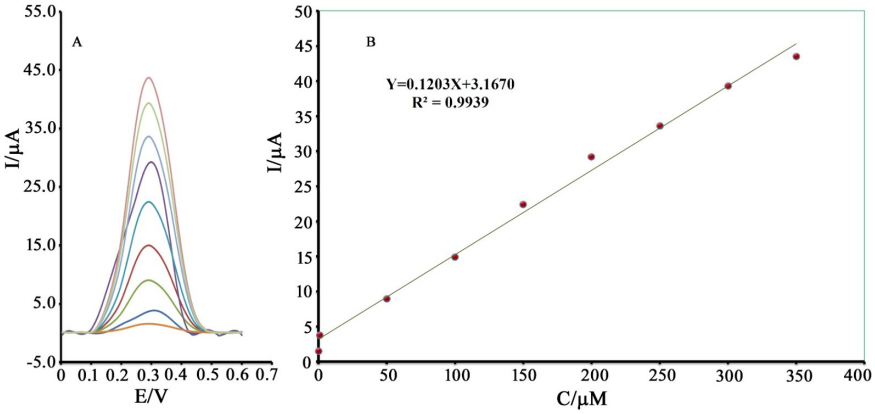

Figure 9. (A) DP voltammograms vanillin in concentration range 1.0 nM to 350 μM at surface of NiO/SWCNTs/[HMIM][BF_4]/PE in the range 1.0 nM to 350 μM (a-i). (B) Curve of anodic current changes depending on vanillin concentration changes (n = 4).

of vanillin using NiO/SWCNTs/[HMIM][BF_4]/PE using LOD = 3 S_b/m (S_b is standard deviation of the blank signal and m is Slope of the calibration curve) equation. The reported analytical data by NiO/SWCNTs/[HMIM][BF_4]/PE are comparable and many cases better than of reported electrochemical sensors for monitoring of vanillin as showed in Table 1.

3.5 Real sample, selectivity and stability investigations

The Chocolate, Coffee milk and biscuits were selected as vanillin-containing samples and after initial preparation according to the route presented in section 2.3, they were introduced into the electrochemical cell and their vanillin content was determined using the standard addition method and the designed sensor. The vanillin content in real samples was also determined using the HPLC method [47] and the data obtained by the two methods are compared in Table 2. As can be seen, the results obtained from both methods are very close to each other and confirm the capability of the sensor.

The effect of potential coexisting species on the electrochemical detection of 10 μM vanillin using NiO/SWCNTs/[HMIM][BF_4]/PE was systematically evaluated under optimized conditions. The tolerance threshold was defined as the highest concentration of an interfering substance that produced less than a ±5% deviation in the measured vanillin response. Experimental findings revealed that the presence of glucose, and ethanol at concentrations up to 800 times greater than vanillin did not compromise detection accuracy. Similarly, Mg^{2+}, SO_4^{2-}, Ca^{2+}, Li^{+}, and F^{-} were tolerated at 1000-fold excess, while urea and uric acid were acceptable at 200-fold levels. Amino acids such as glycine, methionine, as well as phenylalanine, showed no significant interference at 300-fold excess. In addition, caffeic acid, gallic acid and ferulic acids showed no significant interference at 100-fold excess. The results clearly confirm good selectivity of NiO/SWCNTs/[HMIM][BF_4]/PE as new analytical sensor for monitoring of vanillin.

Sensor stability is critical performance indicator in evaluation of new analytical tool. In this study, the NiO/SWCNTs/[HMIM][BF_4]/PE retained its functionality after being stored at 4 °C for six weeks, exhibiting only a slight reduction in peak current response. For 100 μM vanillin, the relative standard deviation (RSD) was determined to be 2.9%, confirming the excellent stability of the new sensor. To evaluate the reproducibility of the NiO/SWCNTs/[HMIM][BF_4]/PE, five independent electrodes were fabricated under identical conditions and tested in the presence of 50 μM vanillin.

The relative standard deviation (RSD) of the peak current response was calculated to be 2.4%, while the RSD of the corresponding potential was 1.1%. These low RSD values confirm that the electrode preparation procedure is highly reproducible, ensuring reliable performance for practical applications.

Table 2. Analysis of vanillin in real samples using suggested sensor and HPLC methods.

Sample	Added (μM)	Expected (μM)	Founded (suggested sensor) (μM)	Founded (HPLC method) (μM) [47]
biscuits	-	-	4.11 ± 0.28	3.99 ± 0.54
	10.00	14.11	14.00 ± 0.57	14.34 ± 0.63
Coffee milk	-	-	3.55 ± 0.34	3.63 ± 0.65
	10.00	13.63	13.75 ± 0.61	13.77 ± 0.73
Chocolate	-	-	1.50 ± 0.18	1.45 ± 0.26
	10.00	11.50	11.68 ± 0.34	11.35 ± 0.69

4. Conclusion

In this study, we successfully developed a high-sensitivity electrochemical sensor for vanillin measurement using a novel modification of carbon paste electrodes with NiO/SWCNTs nanocomposite and the ionic liquid [HMIM][BF_4]. The synergistic effects of these modifications significantly enhanced the sensor's performance, resulting in a 3.22-fold increase in oxidation current and a reduction of 225 mV in oxidation overvoltage. The optimization of critical parameters, including catalyst ratios and buffer conditions, led to the establishment of ideal conditions for effective vanillin detection. The sensor demonstrated a low detection limit of 0.3 nM and showcased reliable performance in analyzing real food samples, such as chocolate, coffee milk, and biscuits, with results closely matching those obtained from HPLC methods. Overall, the findings highlight the potential of the NiO/SWCNTs/[HMIM][BF_4]/PE sensor as a practical tool for food safety monitoring, providing an efficient and sensitive approach to quantifying vanillin in various food products. This advancement not only contributes to food quality control but also emphasizes the importance of innovative electrochemical methods in environmental and food analysis.

Authors Contribution
All authors assisted to the conceptualization, literature review, experimental work, data sample analysis, as well as writing, formatting, and editing of the manuscript.

Availability of data and materials
The data that support the findings of this study are available from the corresponding author, upon reasonable request.

Conflict of interests
The authors declare that they have no known competing financial interests or personal relationships that could have appeared to influence the work reported in this paper.

References

[1] A. Cooke. "Dietary food-additive phosphate and human health outcomes". *Compr Rev Food Sci Food Saf*, **16**:906–1021, 2017.

[2] H. Walls, P. Baker, E. Chirwa, and B. Hawkins. "Food security, food safety & healthy nutrition: are they compatible?". *Global Food Secur*, **21**(69-71), 2019.

[3] Zhang C. Long Y. Chen Q. Zhang W. Wu, L. and G. Liu. "Food additives: From functions to analytical methods". *Crit Rev Food Sci Nutr*, **62**:8497–8517, 2022.

[4] F.C. Martins, M.A. Sentanin, and D. De Souza. "Categories of food additives and analytical techniques for their determination. In: Innovative Food Analysis ". Academic Press. Elsevier:123–156, 2021.

[5] T. Sugimura. "Food and cancer". *Toxicol*, **181**:17–21, 2002.

[6] L. Keivanfar, L. Nateghi, L. Rashidi, R. Pourahmad, and H. Rashidi Nodeh. "Comparing two different extraction techniques on chemical composition and antioxidant property of three essential oils of Ferulago contracta, Rosmarinus officinalis and Lavendula sublepoidota". *J Food Meas Charact*, **17**:3579–3591, 2023.

[7] M.B. Hocking. "Vanillin: Synthetic flavoring from spent sulfite liquor". *J Chem Educ*, **74**:1055, 2025.

[8] N.J. Walton, M.J. Mayer, and A. Narbad. "Vanillin". *Phytochem*, **63**: 505–515, 2003.

[9] S. Durant and P. Karran. "Vanillins-a novel family of DNA-PK inhibitors". *Nucleic Acids Res*, **31**:5501–5512, 2003.

[10] J. Burri, M. Graf, P. Lambelet, and J. Löliger. "Vanillin: More than a flavouring agent-a potent antioxidant". *J Sci Food Agric*, **48**:49–56, 1989.

[11] W. Jiang, X. Chen, Y. Feng, J. Sun, Y. Jiang, W. Zhang, F. Xin, and M. Jiang. "Current status, challenges, and prospects for the biological production of vanillin". *Ferment*, **9**:389, 2023.

[12] A. Mirani and M. Goli. "Optimization of cupcake formulation by replacement of wheat flour with different levels of eggplant fiber using response surface methodology". *Food Sci. Technol*, **42**:e52120, 2021.

[13] N. Ahmadi, M. Ghavami, L. Rashidi, M. Gharachorloo, and L. Nateghi. "Effects of adding green tea extract on the oxidative stability and shelf life of sunflower oil during storage". *Food Chem X*, **21**:101168, 2024.

[14] F. Farokhian, M. Jafarpour, M. Goli, and O. Askari-Khorasgani. "Quality preservation of air-dried sliced button mushroom (Agaricus bisporus) by lavender (*Lavendula angustifolia mill.*) essential oil". *J Food Process Eng*, **40**:12432, 2017.

[15] Y. Ni, G. Zhang, and S. Kokot. "Simultaneous spectrophotometric determination of maltol, ethyl maltol, vanillin and ethyl vanillin in foods by multivariate calibration and artificial neural networks". *Food Chem.*, **89**:465–473, 2005.

[16] K.N. Waliszewski, V.T. Pardio, and S.L. Ovando. "A simple and rapid HPLC technique for vanillin determination in alcohol extract". *Food Chem*, **101**:1059–1062, 2007.

[17] J. Peng, C. Hou, and X. Hu. "A graphene-based electrochemical sensor for sensitive detection of vanillin". *Int J Electrochem Sci*, **7**: 1724–1733, 2012.

[18] H. Gholizadeh, A. Ghorbani-HasanSaraei, H. Tahermansouri, and S.A. Shahidi. "The simultaneous adsorption and desorption of flavonoids from bitter orange peel by the carboxylated multi-walled carbon nanotubes.". *Carbon Lett*, **29**:273–279, 2019.

[19] N. Zare, H. Karimi-Maleh, Z. Zhang, L. Fu, J. Rouhi, N. Zhong, Y. Wen, and M. Ghalkhani. "Enhancing cancer biomarker identification: precise monitoring of MUC1 using V2C/Au nanocomposite-amplified electrochemical biosensor". *Carbon Lett*, **35**:1691–1700, 2025.

[20] L. Jia, Z. Lei, N. Zare, T. Wu, M. Ghalkhani, L. Wan, and Y. Xu. "Ti_3C_2 MXene-enhanced Electrochemical Biosensors for Prostate-Specific Antigen (PSA) Detection in Prostate Cancer". *J Nanostruct Chem*, **15**:1–10, 2024.

[21] G. Wang, G. Leng, and J. Cao. "Electrochemical detection of procaine hydrochloride anesthetic using diamond-graphene composite electrodes". *Alexandria Eng J*, **120**:229–236, 2025.

[22] L. Huang, K. Hou, X. Jia, H. Pan, and M. Du. "Preparation of novel silver nanoplates/graphene composite and their application in vanillin electrochemical detection". *Mater Sci Eng C*, **38**:39–45, 2014.

[23] L. Fu, K. Xie, D. Wu, A. Wang, H. Zhang, and Z. Ji. "Electrochemical determination of vanillin in food samples by using pyrolyzed graphitic carbon nitride". *Mater Chem Phys*, **242**:122462, 2020.

[24] S. Cheraghi, M.A. Dasar, and M.A. Taher. "Fe_3O_4/RGO-ionic liquid nanocatalyst as amplifier for fabrication of highly sensitive electrochemical sensor in monitoring of thallium environmental fluids". *J Nanostruct Chem*, **15**:1–10, 2025.

[25] K. Zhang, Z. Zhao, J. Huang, H. Fu, S. Jiang, and M. Shi. "Fabrication of graphene/MoS_2 composite material for enhanced electrochemical sensing of carcinoembryonic antigen in lung cancer detection". *Alexandria Eng J*, **128**:1219–1230, 2025.

[26] A.F. Putra, A.S. Ningrum, S. Suyanto, V.M. Pratiwi, M.Y.H. Widianto, I. Irkham, W.T. Wahyuni, I. Rahmawati, F.M. Wang, C.H. Huang, and R.A. Wahyuono. "Monolayer graphene/platinum-modified 3D origami microfluidic paper-based biosensor for smartphone-assisted biomarkers detection". *ADMET DMPK*, **13**: 1–17, 2025.

[27] S. Bhagat, J.A. Buled, A.R. Solangi, A. Mallah, and S.T.H. Sherazi. "Fabrication of Bi_2O_3/rGO nanocomposite: A high-performance electrochemical sensor for cadmium detection in industrial wastewater". *J Nanostruct Chem*, **15**:1–13, 2025.

[28] Z. Yang, X. Chen, M. Liao, F. Liao, W. Chen, Q. Shao, B. Liu, and D. Sun. "Label-free electrochemical aptasensing of cardiac cell secretomes in cell culture media for evaluation of drug-induced myocardial injury". *J Pharm Anal*, 2025.

[29] O. Moradi. "A review on nanomaterial-based electrochemical sensors for determination of vanillin in food samples". *Food Chem Toxicol*, **168**:113391, 2022.

[30] M. Mostofi, M. Ebrahimi, and S.A. Beyramabadi. "Ultrasensitive monitoring of idarubicin in environmental and biological fluids using amplification of electrochemical sensor with NiO–SWCNTs/CNT nanocomposites and 1-ethyl-3-methylimidazolium chloride conductive catalysts". *Carbon Lett*, **34**:797–803, 2024.

[31] Y. Xu, S.W. Wang, H. Bagheri, C. Chen, and Y. Zhou. "Innovative TiVC/dsDNA biosensor platform for enhanced detection of anastrozole: Experiment and DFT approaches". *Alexandria Eng J*, **129**: 1146–1152, 2025.

[32] A. Chen and S. Chatterjee. "Nanomaterials based electrochemical sensors for biomedical applications". *Chem Soc Rev*, **42**:5425–5438, 2013.

[33] B. Li, X. Xie, T. Meng, X. Guo, Q. Li, Y. Yang, H. Jin, C. Jin, X. Meng, and H. Pang. "Recent advance of nanomaterials modified electrochemical sensors in the detection of heavy metal ions in food and water". *Food Chem*, **440**:138213, 2024.

[34] L.G. Sutanto, S. Sabilla, B.Y. Wardhana, A. Ramadani, A.P. Sari, Q.K. Anjani, W.J. Basirun, T. Amrillah, I. Amalina, and P.K Jiwanti. "Carbon nanomaterials as electrochemical sensors for theophylline: A review". *RSC Adv*, **14**:28927–28942, 2023.

[35] T. Wu, Y. Li, Z. Zhang, D. Zhang, E.N. Dragoi, and H. Karimi-Maleh. "3D print-based polypyrrole/TiVCTx/UiO-66 composites for effective adsorption of combined pollutants in water media". *J Nanostruct Chem*, **15**:1–23, 2025.

[36] P. Kannan and G. Maduraiveeran. "Metal oxides nanomaterials and nanocomposite-based electrochemical sensors for healthcare applications". *Biosensors*, **13**:542, 2023.

[37] A. Hosseinian-Roudsari, S.A. Shahidi, A. Ghorbani-HasanSaraei, S. Hosseini, and F. Fazeli. "A new electroanalytical approach for sunset yellow monitoring in fruit juices based on a modified sensor amplified with nanocatalyst and ionic liquid". *Food Chem Toxicol*, **168**:113362, 2022.

[38] J. Arjmandi, S.A. Shahidi, A. Ghorbani-HasanSaraei, M.B. Limooei, and S.N. Raeisi. "Sudan I monitoring as a hazardous azo dye using an electroanalytical tool amplified with NiO/SWCNTs–ionic liquid catalysts". *Chemosphere*, **309**:136673, 2022.

[39] I. Kouhi, G. Parvizi Fard, E. Alipour, and A. Saadatirad. "Development of an electrochemical sensor for determination of vanillin in some food stuffs". *J Food Process Preserv*, **46**:e16289, 2022.

[40] C. Raril and J. Manjunatha. "A simple approach for the electrochemical determination of vanillin at ionic surfactant modified graphene paste electrode". *Microchem J*, **154**:104575, 2020.

[41] M. Abbasghorbani. "Electrochemical determination of vanillin in food samples using MgO/SWCNTs–ionic liquid modified electrode". *Int J Electrochem Sci*, **12**:11656–11665, 2017.

[42] V.K. Gupta, H. Karimi-Maleh, S. Agarwal, F. Karimi, M. Bijad, M. Farsi, and S.A. Shahidi. "Fabrication of a food nano-platform sensor for determination of vanillin in food samples". *Sensors*, **18**: 2817, 2018.

[43] P. Deng, Z. Xu, R. Zeng, and C. Ding. "Electrochemical behavior and voltammetric determination of vanillin based on an acetylene black paste electrode modified with graphene–polyvinylpyrrolidone composite film". *Food Chem*, **180**:156–163, 2015.

[44] J. Peng, C. Hou, and X. Hu. "A graphene-based electrochemical sensor for sensitive detection of vanillin". *Int J Electrochem Sci*, **7**: 1724–1733, 2012.

[45] J. Peng, L. Wei, Y. Liu, W. Zhuge, Q. Huang, W. Huang, G. Xiang, and C. Zhang. "Novel porous iron phthalocyanine-based metal–organic framework electrochemical sensor for sensitive vanillin detection". *RSC Adv*, **10**:36828–36835, 2020.

[46] A.J. Bard, L.R. Faulkner, and H.S. White. "Electrochemical methods: fundamentals and applications". John Wiley & Sons, 2022.

[47] E. Pérez-Esteve, M.J. Lerma-García, A. Fuentes, C. Palomares, and J.M. Barat. "Control of undeclared flavoring of cocoa powders by determination of vanillin and ethyl vanillin by HPLC". *Food Control*, **67**:171–176, 2016.